Non-adiabatic transition of the fissioning nucleus at scission: the time scale

N. Carjan[1,2], M. Rizea[2]

[1] **Centre d'Etudes Nucléaires de Bordeaux - Gradignan, UMR 5797, CNRS/IN2P3 - Université Bordeaux 1, BP 120, 33175 Gradignan Cedex, France**

[2] **"Horia Hulubei" National Institute of Physics and Nuclear Engineering, Bucharest, Romania**

Introduction

Time-dependent approach to the fast transition at scission:
$\{\alpha^i\} \rightarrow \{\alpha^f\}$; *i and f meaning just-before and immediately-after*.
"New" scission model:
1) dynamical: it takes into account the duration of the neck rupture and its integration in the fragments
2) microscopic: it calculates the time evolution of each occupied neutron state
3) fully quantum mechanical: it uses the two-dimensional time-dependent Schrödinger equation (TDSE2D) with time-dependent potential (TDP).
Most previous models were statical, statistical and semiclassical: Fong (1963), Wilkins et al. (1976), etc.
The picture behind the present model was first proposed by Fuller (Wheeler) in 1962 and illustrated by a "volcano erupting" in the middle of a Fermi sea.

Plan

- Presentation of the model.
- Numerical solution of TDSE2D with TDP.
- Application to the scission process: focus on single-particle excitations.
- Formalism: excitation energy of the nascent fission fragments, multiplicity of the neutrons released at scission, distribution of their emission points and finally the partition of these quantities among the fission fragments.
- Numerical results for ^{236}U.
- Summary.

N. Carjan, M. Rizea, Phys. Rev C 82 (2010) 014617

'sudden approximation'

Halpern's cartoon

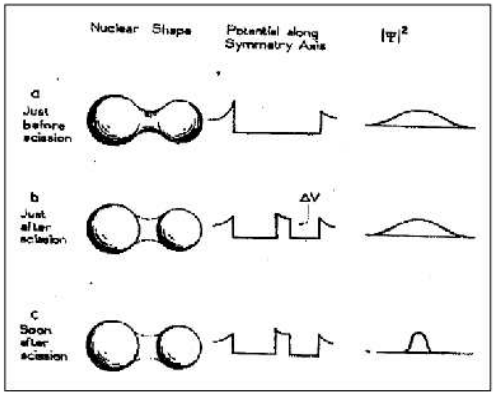

Equipotential lines $V_0/2$ for the pre and post scission configurations studied in this work

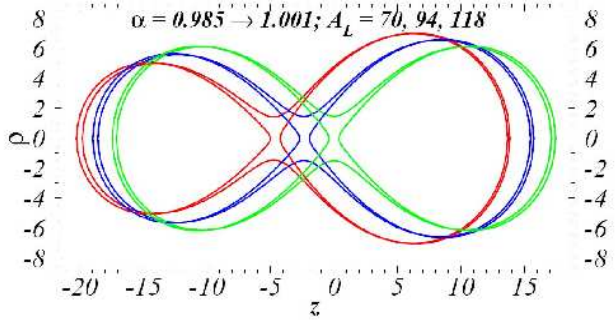

N. Carjan, P. Talou, O.Serot, Nucl.Phys. A792 (2007) 102.

Model

Mechanism for excitation and emission of neutrons during the last stage of nuclear fission: coupling between the neutron degree of freedom and the rapidly changing potential of its interaction with the rest of the nucleus.
A realistic mean field is used: Woods-Saxon type with spin-orbit term adapted to nuclear shapes described by Cassini ovals.
The numerical method used to solve TDSE2D with TDP is unconditionally stable (it doesn't rely on the alternating direction approximation) and avoids reflections on the numerical boundary.
The duration of the neck rupture and its absorption T is taken as parameter in the interval [0.25,9.00]$\times 10^{-22}$ sec.

Time-dependent Schrödinger equation

The equation that describes the motion of a nucleon in an axially symmetric deformed nucleus has the form

$$i\hbar\frac{\partial\Psi(\rho,z,\phi,t)}{\partial t}=\mathcal{H}(\rho,z,\phi,t)\Psi(\rho,z,\phi,t). \qquad (1)$$

In cylindrical cordinates, the wavefunction has two components, corresponding to spin up and down:

$$\Psi(\rho,z,\phi,t)=f_1(\rho,z,t)e^{i\Lambda_1\phi}|\uparrow\rangle+f_2(\rho,z,t)e^{i\Lambda_2\phi}|\downarrow\rangle, \qquad (2)$$

where $\Lambda_1=\Omega-\frac{1}{2},\ \Lambda_2=\Omega+\frac{1}{2}$ and Ω is the projection of the total angular momentum along the symmetry axis. Due to the axial symmetry, ϕ disappears and we have:

The Hamiltonian

$$\mathcal{H}\Psi = \begin{bmatrix} O_1 - CS_c & -CS_a \\ -CS_b & O_2 - CS_d \end{bmatrix} \begin{bmatrix} f_1 \\ f_2 \end{bmatrix}, \qquad (3)$$

$$O_{1,2} = -\frac{\hbar^2}{2\mu}(\Delta - \frac{\Lambda_{1,2}^2}{\rho^2}) + V(\rho, z, t), \quad \Delta = \frac{1}{\rho}\frac{\partial}{\partial\rho} + \frac{\partial^2}{\partial\rho^2} + \frac{\partial^2}{\partial z^2}.$$

Δ is the Laplacean, V is the potential, C is a const. and the operators $S_a, \ldots, S_d$ represent the spin-orbit coupling. The nucl.shape is described in terms of Cassini ovaloids. This representation depends on a set of param.; in our case we considered two: α (elongation) and α_1 (mass asymmetry). By the transform. $g_{1,2} = \rho^{1/2} f_{1,2}$ (Liouville), the 1st deriv. from Δ is removed, resulting a simplified Hamiltonian $\hat{\mathcal{H}}$ with w.f. $\hat{\Psi}$ having the components g_1, g_2:

The Transformed Hamiltonian

$$\hat{\mathcal{H}}\hat{\Psi} = \begin{bmatrix} L_1 + P_c & P_- \\ P_+ & L_2 + P_d \end{bmatrix} \begin{bmatrix} g_1 \\ g_2 \end{bmatrix},$$

$$L_{1,2} = -\frac{\hbar^2}{2\mu}\left(\frac{\partial^2}{\partial\rho^2} + \frac{\partial^2}{\partial z^2} + \frac{1/4 - \Lambda_{1,2}^2}{\rho^2}\right) + V(\rho, z, t),$$

$$P_\pm = \pm Q_1 + Q_2,\ Q_1 = C\left(\frac{\partial V}{\partial\rho}\frac{\partial}{\partial z} - \frac{\partial V}{\partial z}\frac{\partial}{\partial\rho}\right),\ Q_2 = C\frac{\Omega}{\rho}\frac{\partial V}{\partial z},$$

$$P_c = -C\frac{\Lambda_1}{\rho}\frac{\partial V}{\partial\rho}, P_d = C\frac{\Lambda_2}{\rho}\frac{\partial V}{\partial\rho}.$$

TDSE is solved by a Crank-Nicolson scheme ($\hat{\mathcal{H}}' = \frac{\partial\hat{\mathcal{H}}}{\partial t}$):

$$\left(1 + \frac{i\Delta t}{2\hbar}\hat{\mathcal{H}} + \frac{i\Delta t^2}{4\hbar}\hat{\mathcal{H}}'\right)\hat{\Psi}(t+\Delta t) = \left(1 - \frac{i\Delta t}{2\hbar}\hat{\mathcal{H}} - \frac{i\Delta t^2}{4\hbar}\hat{\mathcal{H}}'\right)\hat{\Psi}(t).$$

The definition of the potential

The nuclear potential is given by

$$V_N(\rho, z) = -V_0 \left[1 + \exp(\Theta/a)\right]^{-1} \tag{4}$$

where V_0 is the depth and a the diffuseness. The quantity Θ is an approx. to the distance between a point and the nuclear surface, described by Cassini ovals. The spin-orbit interaction is taken proportional to the gradient of V_N:

$$V_{so} = -C[\bar{\boldsymbol{\sigma}} \times \bar{\boldsymbol{p}}]\nabla V_N, \quad C = \lambda \left(\frac{\hbar}{2\mu c}\right)^2 \tag{5}$$

where $\bar{\boldsymbol{\sigma}}$ and $\bar{\boldsymbol{p}}$ are the nucleon spin and momentum. The constant C involves the strength of the spin-orbit interaction.

The spatial discretization

For numerical solving, the infinite physical domain should be limited to a finite one, $[0, R] \times [-Z, Z]$, which is discretized by a grid with the mesh points: $\rho_j = j\Delta\rho$, $1 \leq j \leq J$ $(\rho_J = R)$, $z_k = k\Delta z$, $-K \leq k \leq K$ $(z_K = Z)$. At each point the partial derivatives in $\hat{\mathcal{H}}$ are approximated by finite difference formulas. For the derivatives w.r. to z we used standard 3-point formula, while for the derivatives in ρ, we deduced a special formula, which takes into account the accomplished function transformation. It has the (symmetric) form: $h^2 g_j'' \approx a_j g_{j+1} + b_j g_j + a_j g_{j-1}$, where g is any of the two functions. The coefficients a_j, b_j are determined so that the formula is exact when g is replaced by $\rho^{1/2+\Lambda}$; $\rho^{5/2+\Lambda}$ (the leading terms of its series expansion - the cylind. symm. is also taken into account).

Adapted finite differences

It results:

$$a_j = \frac{4(\Lambda+1)}{j^2(p_j - q_j)},\ b_j = \frac{1}{j^2}\left[\Lambda^2 - \frac{1}{4} - \frac{4(\Lambda+1)q_j}{p_j - q_j}\right], \quad (6)$$

$$p_j = (1+\frac{1}{j})^{\Lambda+\frac{5}{2}} + (1-\frac{1}{j})^{\Lambda+\frac{5}{2}},\ q_j = (1+\frac{1}{j})^{\Lambda+\frac{1}{2}} + (1-\frac{1}{j})^{\Lambda+\frac{1}{2}}.$$

$a_j \to 1, b_j \to -2$ as $j \to \infty$, i.e. the above formula $\to$ the standard one. The variable coeff. are used only in the vicinity of $\rho = 0$, where the particular behavior of g is dominant. In the rest of the interval, the stand.form.is applied. Note that $\hat{\mathcal{H}}$ still contains first derivatives w.r. to ρ (in the spin-orbit components). These deriv.are approximated as well by adapted diff.formulas, deduced in a similar way.

Numerical solution of TDSE

Let us denote $g_{jk}^{(n)}$ the approx. of g in the point (ρ_j, z_k) and at time $t_n = n\Delta t$ (g is any of g_1 and g_2). As initial solution (at $t_0 = 0$) we take an eigenfunction of the stationary Schrödinger equation whose potential corresponds to the starting deformation. We use the same discretization of the Hamiltonian and we arrive to an algebraic eigenvalue problem, which is solved by the package ARPACK, based on the Implicitly Restarted Arnoldi Method. The solution at time t_{n+1}, represented by the values $g_{jk}^{(n+1)}$, is obtained in terms of the solution at time t_n, on the basis of the above CN scheme, which turns into a linear system, after the discretization. It is solved by the conjugate gradient iterative method.

Transparent Boundary Conditions

Special cond. on the boundaries of the comput. domain should be imposed to avoid the reflexions which alter the propagated w.f. We implemented a variant of transparent bound.cond. The idea is to assume near the boundary r_B the following form of the sol.:$g = g_0 \exp(ik_r r)$,$g_0, k_r \in \mathbf{C}$ (a 1D notation was used). Linear relations between g_{B+1} and g_B then result, which are used in the fin.diff.formulas for the derivatives at r_B, when the CN scheme is applied. In 2D, this algorithm should be used at each point of the grid belonging to boundaries. We advance the solution during a temporal interval $[0, T]$. T corresponds to the final configuration. The deform.param. are changing on this interval. At each time step the potential $V(t)$ and its derivative $V'(t)$ are recalculated. This deriv. is obtained by a simple fin.diff.form., using two successive values.

Application to the scission process

A fast transition at scission produces the excitation of all neutrons that are present in the surface region. For few of them, this excitation exceeds their binding and they are released.

Let $|\Psi^i\rangle$, $|\Psi^f\rangle$ be the eigenfunctions corresponding to the just-before-scission and immediately-after-scission configurations respectively. The propagated wave functions $|\Psi^i(t)\rangle$ are wave packets that have also some positive-energy components. The probability amplitude that a neutron occupying the state $|\Psi^i\rangle$ before scission populates a state $|\Psi^f\rangle$ after scission is

$$a_{if} = \langle \Psi^i(T) | \Psi^f \rangle = 2\pi \int \int (g_1^i(T) g_1^f + g_2^i(T) g_2^f) d\rho dz.$$

Excitation energy of the fission fragments

The total occupation probability of a given final eigenstate is:

$$V_f^2 = \sum_{bound} v_i^2 |a_{if}|^2$$

where v_i^2 is the ground-state occupation probability of a given initial eigenstate. Since V_f^2 is different from v_f^2 (the ground-state value), the fragments are left in an excited state. The corresponding excitation energy at scission is:

$$E_{sc}^* = 2 \sum_{bound\ states} (V_f^2 - v_f^2) e_f .$$

The factor of 2 is due to the spin degeneracy.

Occupation probabilities at scission

Consistent with the independent particle model used, $v^2_{i,f}$ are step functions: 1 for states below the Fermi level and 0 above. Possible correlations between neutrons will smooth this function. To see the effect of this modification on the calculated quantities, BCS occupation probabilities are also used:

$$v^2_{i,f} = \frac{1}{2}\left[1 - \frac{e_{i,f} - \lambda}{\sqrt{(e_{i,f} - \lambda)^2 + \Delta^2}}\right],$$

with Δ and λ deduced from the BCS equations. e_i, e_f are the eigen energies of the states $|\Psi^i\rangle$ and $|\Psi^f\rangle$ respectively.

Neutrons emitted at scission

One can also calculate the multiplicity of the neutrons released during scission:

$$\nu_{sc} = 2 \sum_{bound} v_i^2 (\sum_{unbound} |a_{if}|^2).$$

A quantity that influences the amount of neutrons that are reabsorbed, scattered or left unaffected by the fragments and finally determines the angular distribution of the scission neutrons with respect to the fission axis is the spatial distribution of the emission points

$$S_{em}(\rho, z) = \sum_{bound} v_i^2 |\Psi_{em}^i(\rho, z)|^2,$$

where

$$|\Psi^i_{em}\rangle = |\Psi^i(T)\rangle - \sum_{bound\ states} a_{if}|\Psi^f\rangle$$

is the part of the wave packet that is emitted.

Nuclear shapes at scission

The just-before and immediately-after scission configurations are characterized by the parameters $\alpha^i = 0.985$ and respectively, $\alpha^f = 1.001$ in the Cassini description of the nuclear shapes.
The fission can be symmetric (each fragment has the mass 118) or, more frequently, asymmetric. In the latter case, one more deformation parameter, namely α_1, is used. Its value depends on A_L (the light fragment mass) and on α.
To have an idea of the shapes involved we next show the equipotential lines corresponding to half of the depth of the nuclear potential at initial and final deformations for five mass asymmetries.

Equipotential lines $V_0/2$ (before and after scission)

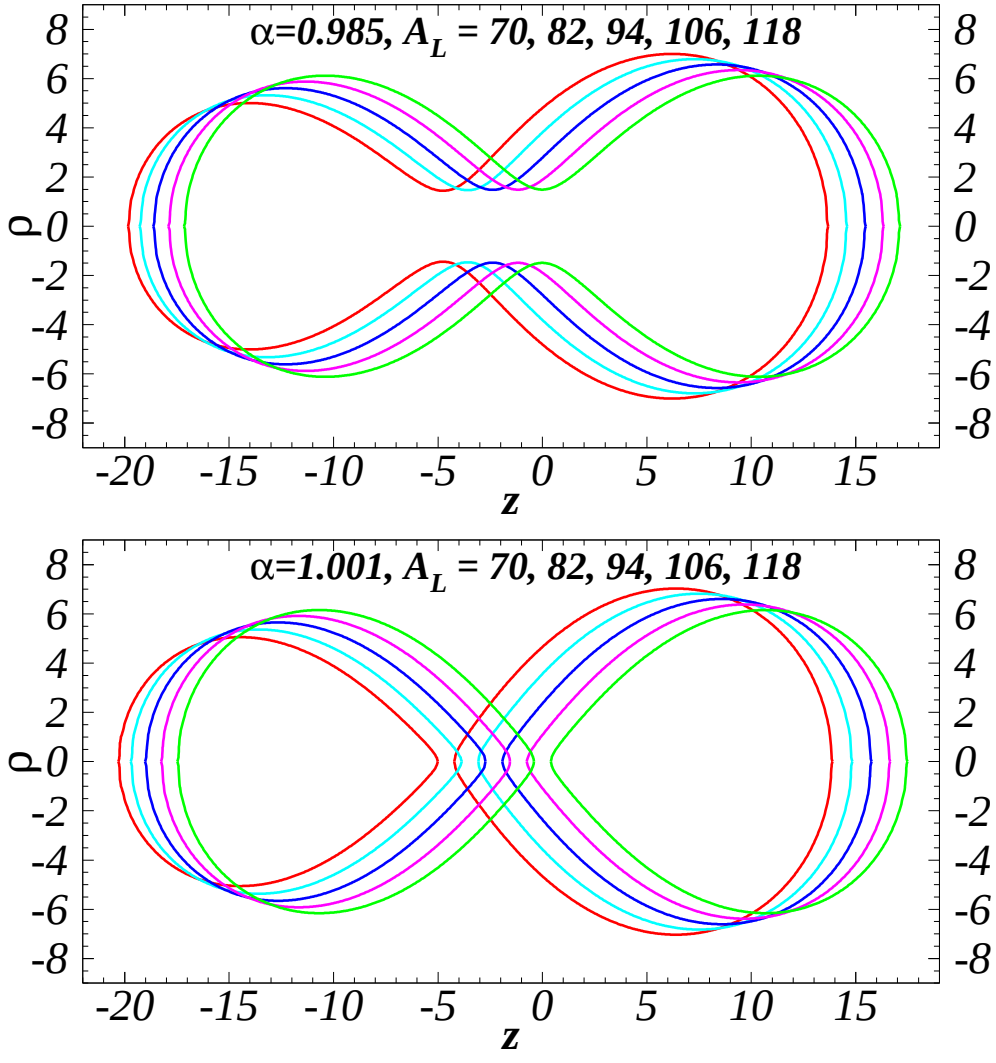

Partition among the fission fragments (1)

Finally it is interesting to separate the contributions of the light (L) and of the heavy (H) fragment using the probability of each emitted (or excited) neutron to be present in the L (or H) fragment:

$$E^*_{sc}(L,H) = \sum_f e_f \left(V_f^2 - v_f^2\right) N_f^{L,H}$$

$$\nu_{sc}(L,H) = \sum_i v_i^2 (\sum_f |a_{if}|^2) N_i^{L,H},$$

where the partial norms $N_{i,f}^{L,H}$ are given by:

Partition among the fission fragments (2)

$$N_{i,f}^{L} = 2\pi \int_0^R \int_{-Z}^{z_{min}} \left[\left(g_1^{i,f} \right)^2 + \left(g_2^{i,f} \right)^2 \right] d\rho dz$$

$$N_{i,f}^{H} = 2\pi \int_0^R \int_{z_{min}}^{Z} \left[\left(g_1^{i,f} \right)^2 + \left(g_2^{i,f} \right)^2 \right] d\rho dz$$

z_{min} corresponds to the neck position, identified as the point between $-Z$ and Z where an equipotential line has a minimum.

The knowledge of E_{sc}^{*}(L,H) is important since it enters into the Monte-Carlo Hauser-Feschbach simulation of the neutron evaporation from the accelerated fragments.

Arbitrary hypotheses concerning the share of excitation energy among the fragments have been employed so far.

Numerical results for ^{236}U

We apply the above formalism to the low energy fission of ^{236}U.

The numerical domain is: $\rho \in [\Delta\rho, 27]$, $z \in [-27, 27]$, while $\Delta\rho = \Delta z = 0.125$. (Number of grid points ≈ 93500). The time step $\Delta t = 1/256 \times 10^{-22}$ sec.

The numerical evaluation of the overlap integrals is performed by the Simpson formula. With respect to ρ the formula is adapted to the special form of the solutions g_1, g_2. Before calculating a_{if}, the eigenfunctions provided by ARPACK are orthonormalized by the Gram-Schmidt algorithm.

Excitation energy as function of transition time T

for T=10^{-22} sec the values are 20% below the sudden limit

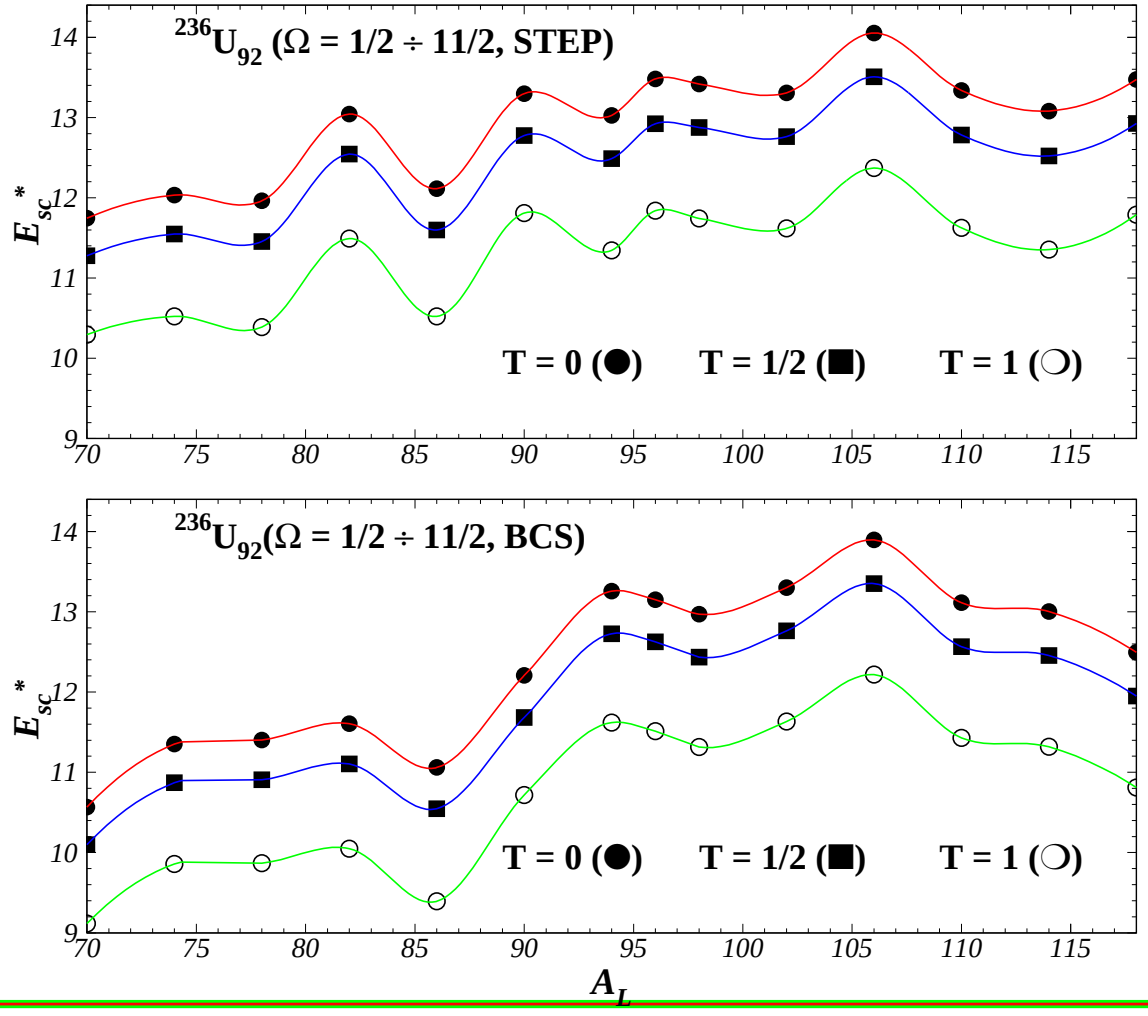

Neutron multiplicity as function of transition time

a smooth occupation-probability function produces little change

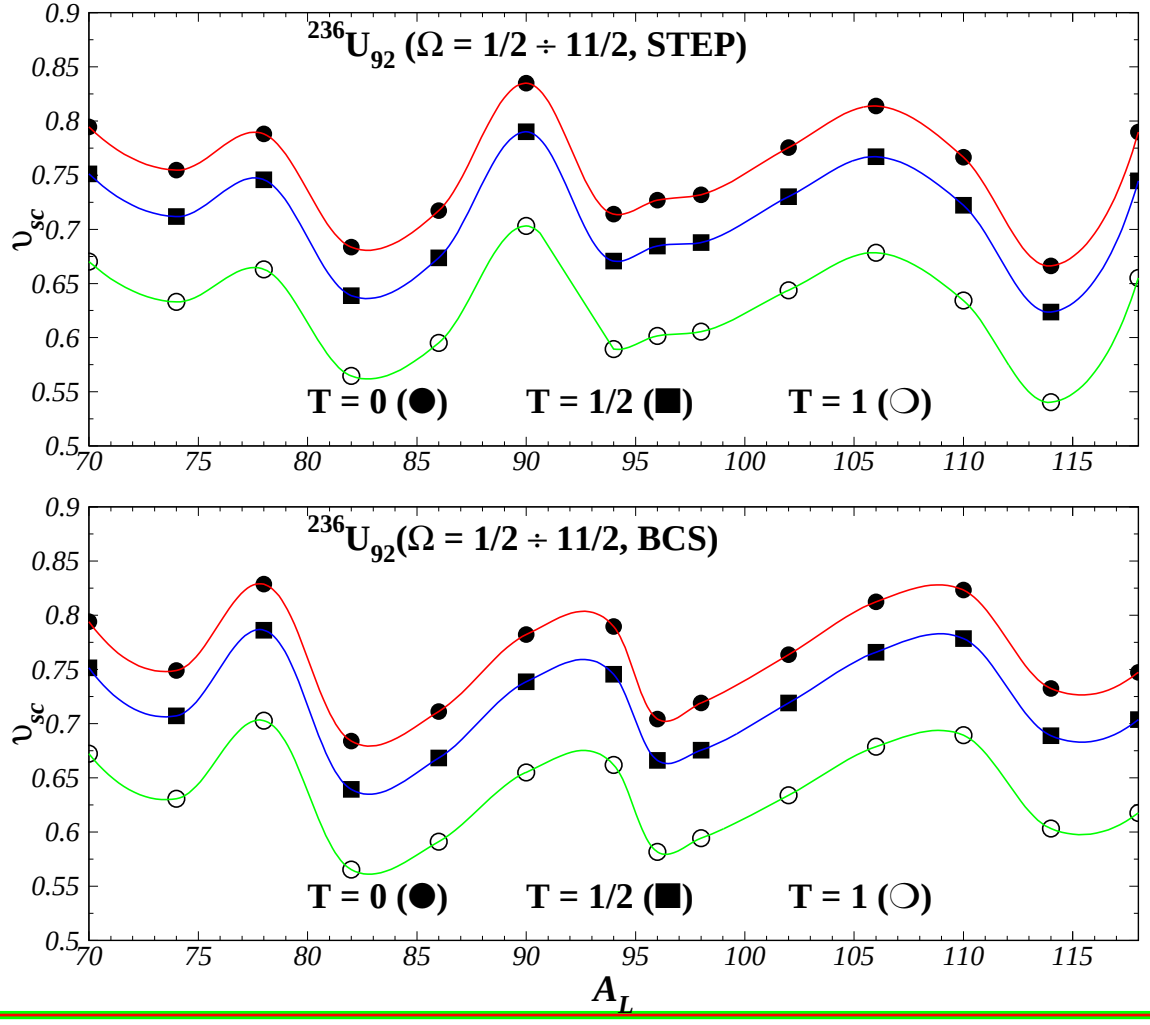

Scission neutron multiplicity

A_L / ΔT	70		90		118	
	ν_{sc}/ **IP**	ν_{sc}/ **PC**	ν_{sc}/ **IP**	ν_{sc}/ **PC**	ν_{sc}/ **IP**	ν_{sc}/ **PC**
0	0.792	0.791	0.833	0.781	0.790	0.747
1/2	0.751	0.751	0.790	0.739	0.745	0.704
1	0.668	0.670	0.704	0.656	0.655	0.618
3	0.290	0.303	0.321	0.298	0.277	0.262
5	0.057	0.080	0.072	0.075	0.051	0.054
6	0.018	0.043	0.025	0.035	0.014	0.019
9	0.020	0.044	0.019	0.032	0.020	0.021

Excitation energy at scission

A_L / ΔT	70		90		118	
	E^*_{sc}/ IP	E^*_{sc}/ PC	E^*_{sc}/ IP	E^*_{sc}/ PC	E^*_{sc}/ IP	E^*_{sc}/ PC
0	11.75	10.57	13.30	12.20	13.48	12.50
1/2	11.28	10.10	12.77	11.68	12.93	11.95
1	10.30	9.121	11.70	10.60	11.79	10.81
3	5.486	4.310	6.461	5.360	6.265	5.318
5	2.145	0.955	2.646	1.557	2.154	1.260
6	1.554	0.351	1.899	0.819	1.336	0.460
9	1.531	0.313	1.831	0.765	1.317	0.438

Emission points (A_L=90; all Ω; T=0,3,5$\times 10^{-22}$sec)

with increasing T the emission points slightly migrate from the H to the L fragment and from the inter-fragment to the inside-fragment regions

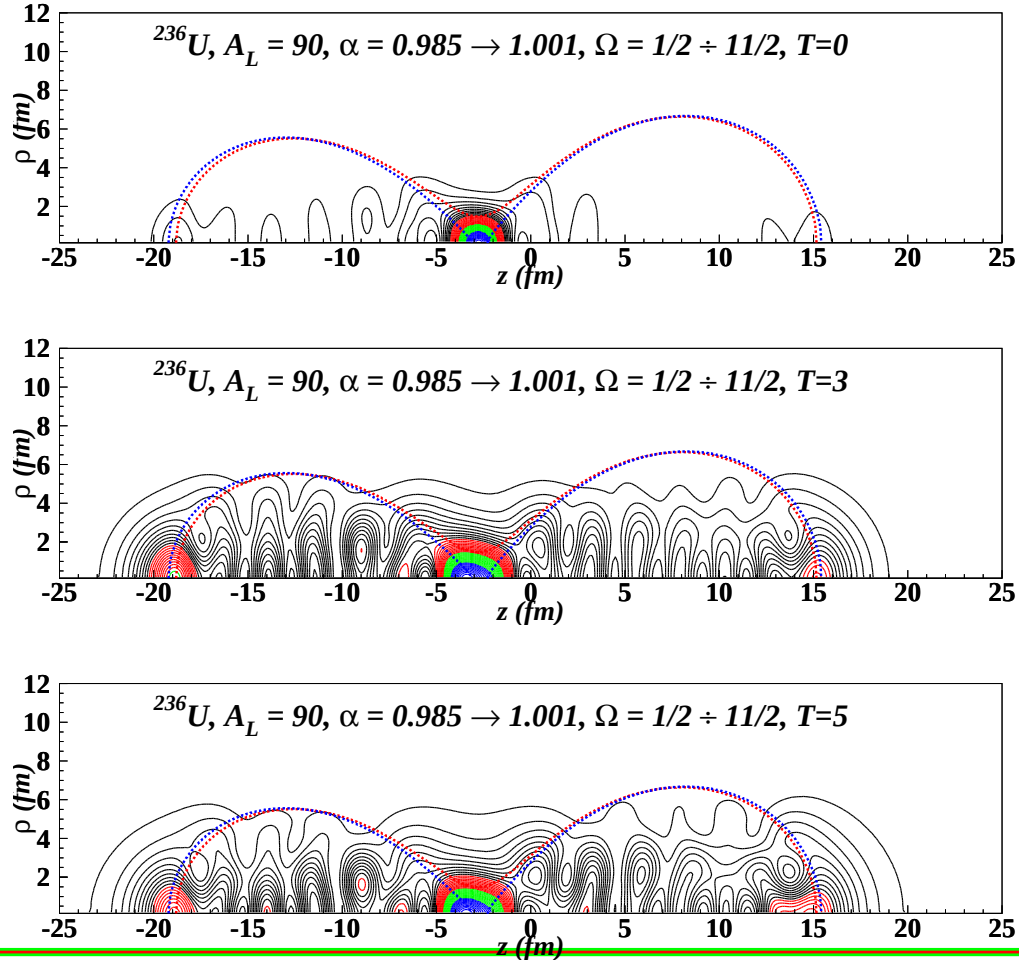

Emission points (A_L=90; T=0; Ω=1/2,3/2,5/2)

neutrons with low Ω values (1/2 and 3/2) are released in the inter-fragment region and have the bigest chance to survive

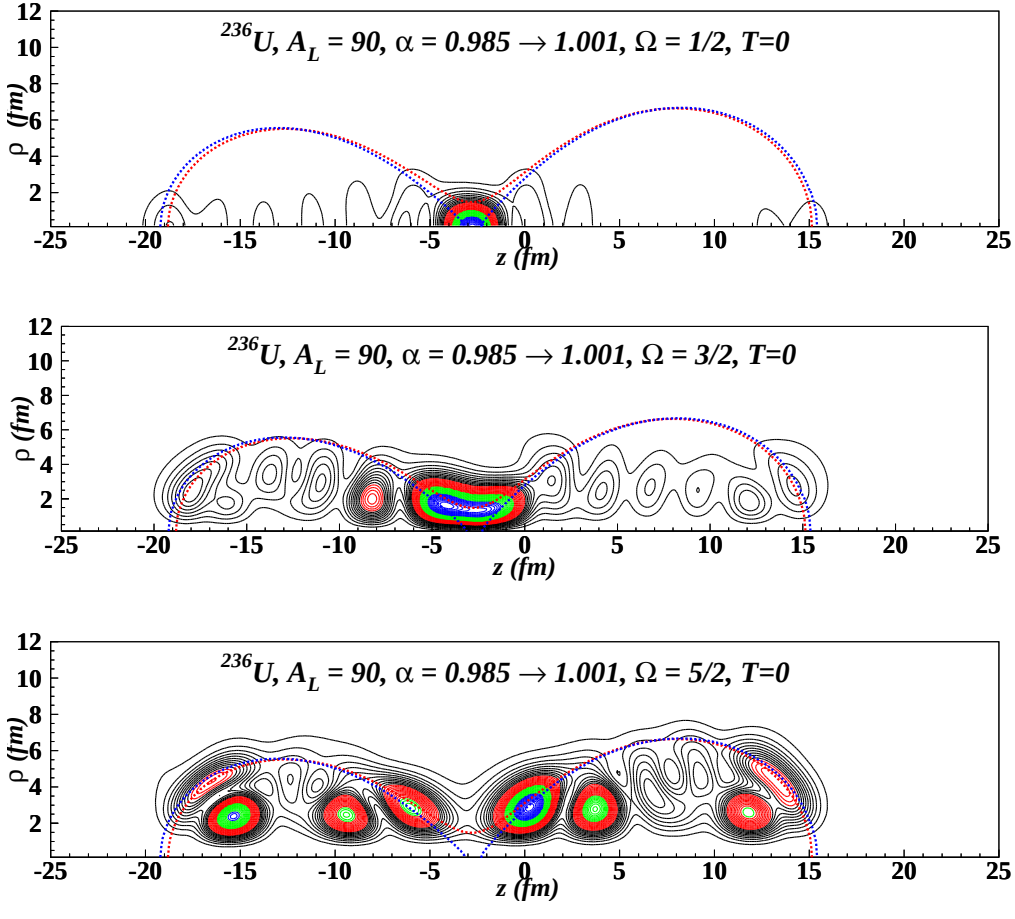

Emission points (A_L=90; T=0; Ω=7/2,9/2,11/2)

neutrons with high Ω values (9/2 and 11/2) are release in the surface region but with very low probability

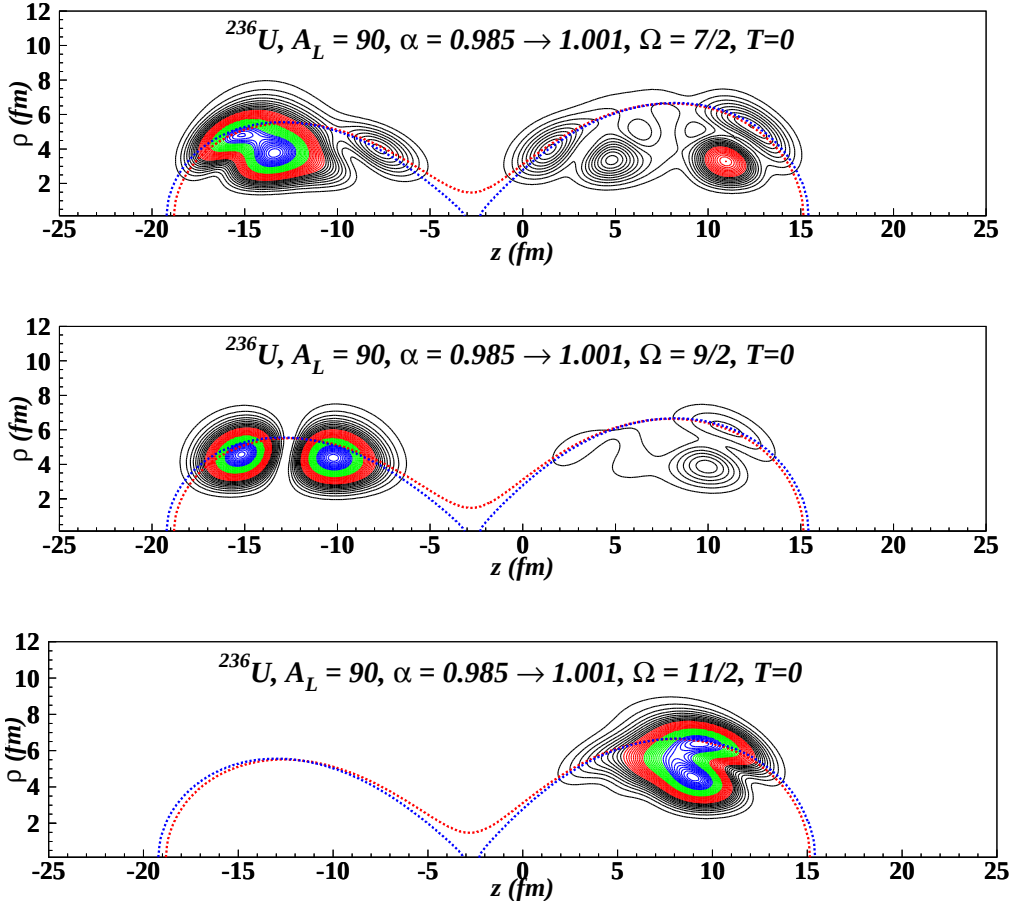

Emission points (A_L=70; all Ω; T=0,1,3,6$\times 10^{-22}$sec)

for this asymmetry the migration from L to H is even more pronounced

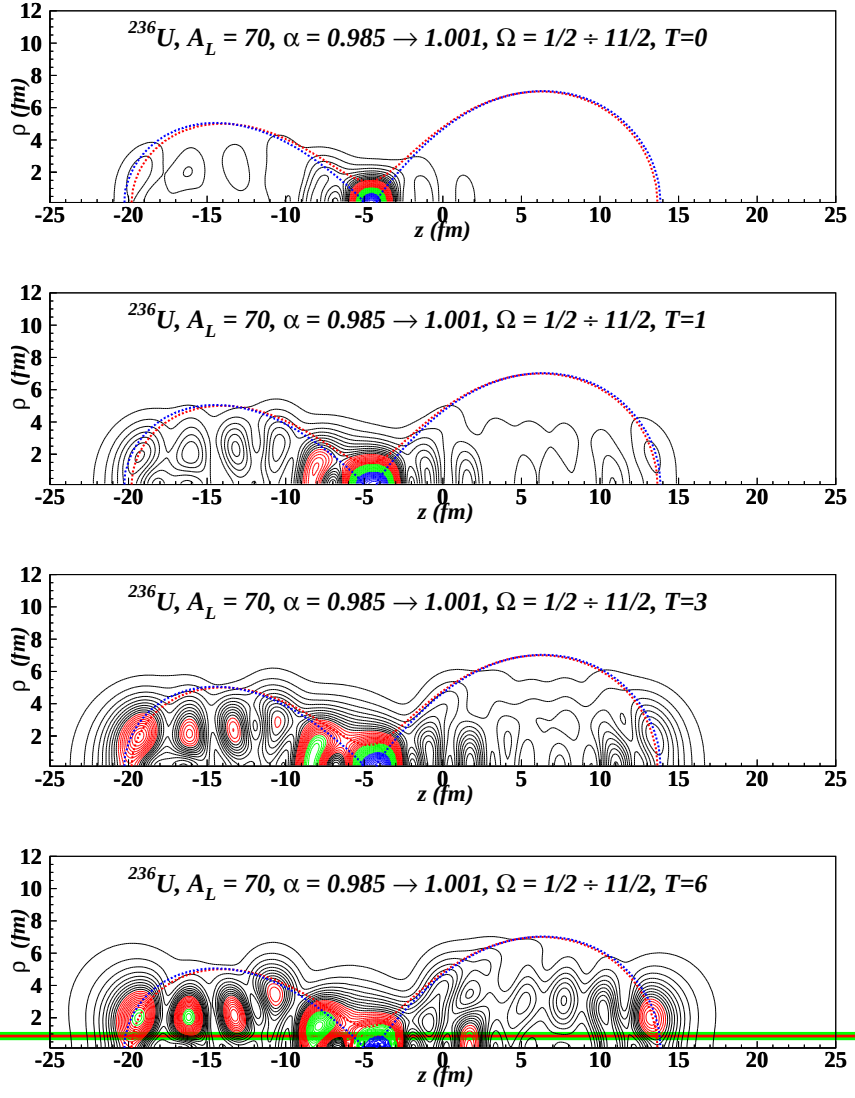

Emission points (A_L=70; T=0; Ω=1/2,3/2,5/2)

Ω=3/2,5/2 are released from the L fragment; Ω=1/2 from the neck

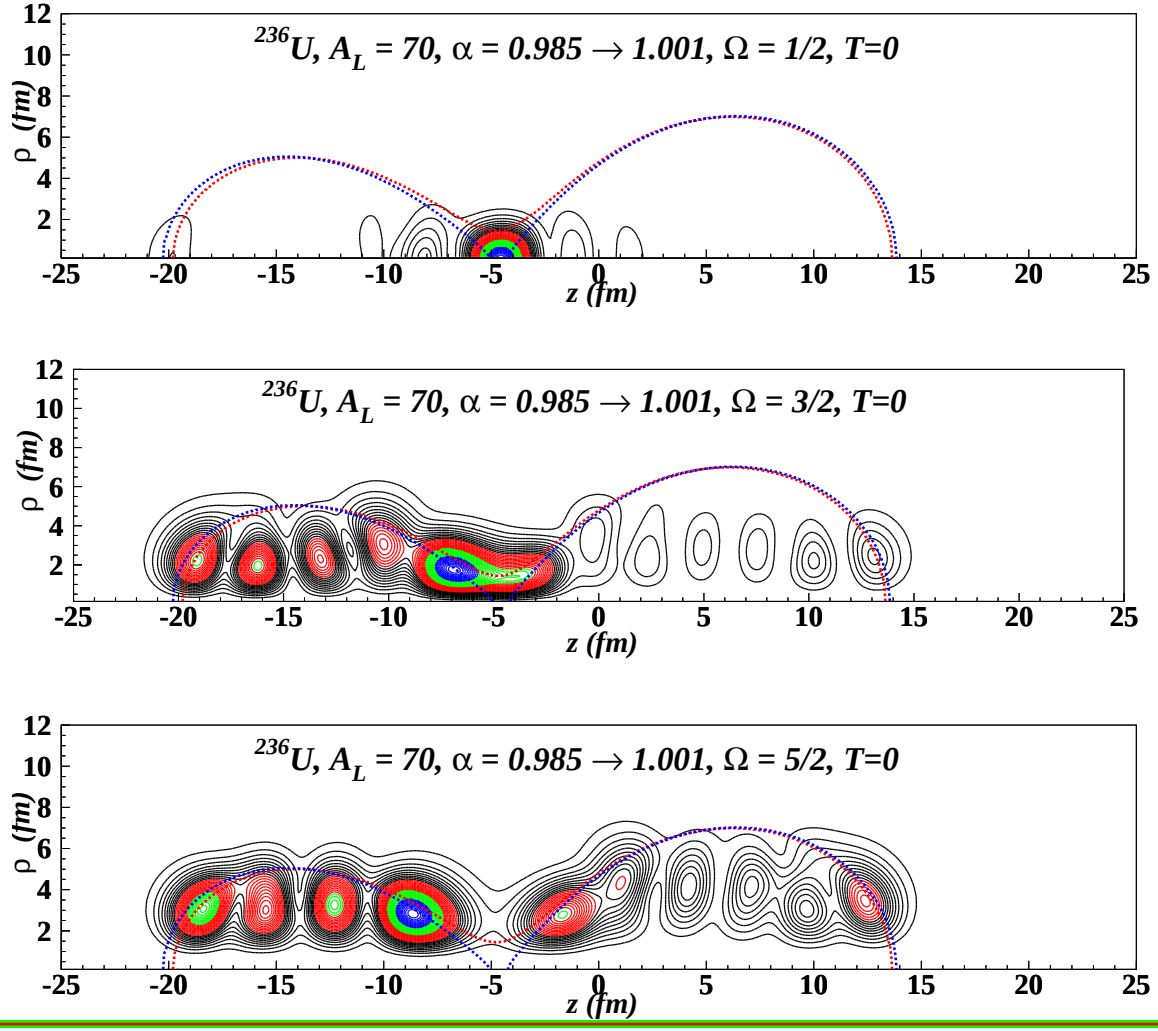

Emission points (A_L=70; T=0; Ω=7/2,9/2,11/2)

high Ω's are released from the H fragment (but with low probability)

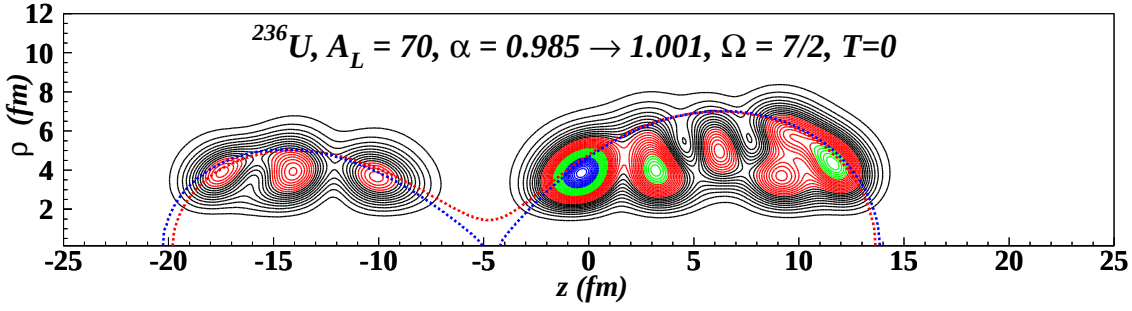

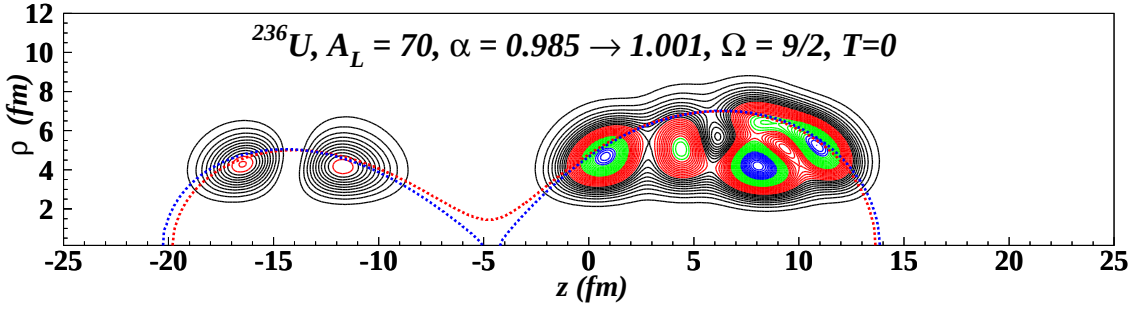

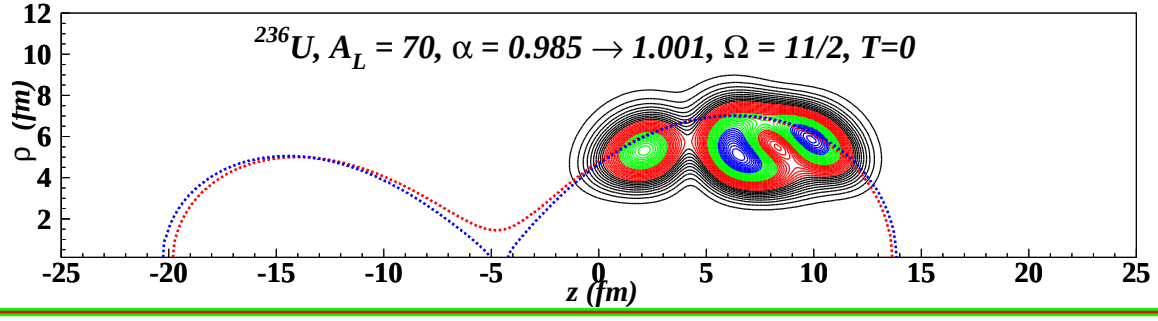

Emission points (A_L=70; T=3; Ω=1/2,3/2,5/2)

For T=3, part of Ω=1/2 states and all Ω=3/2 left the neck region

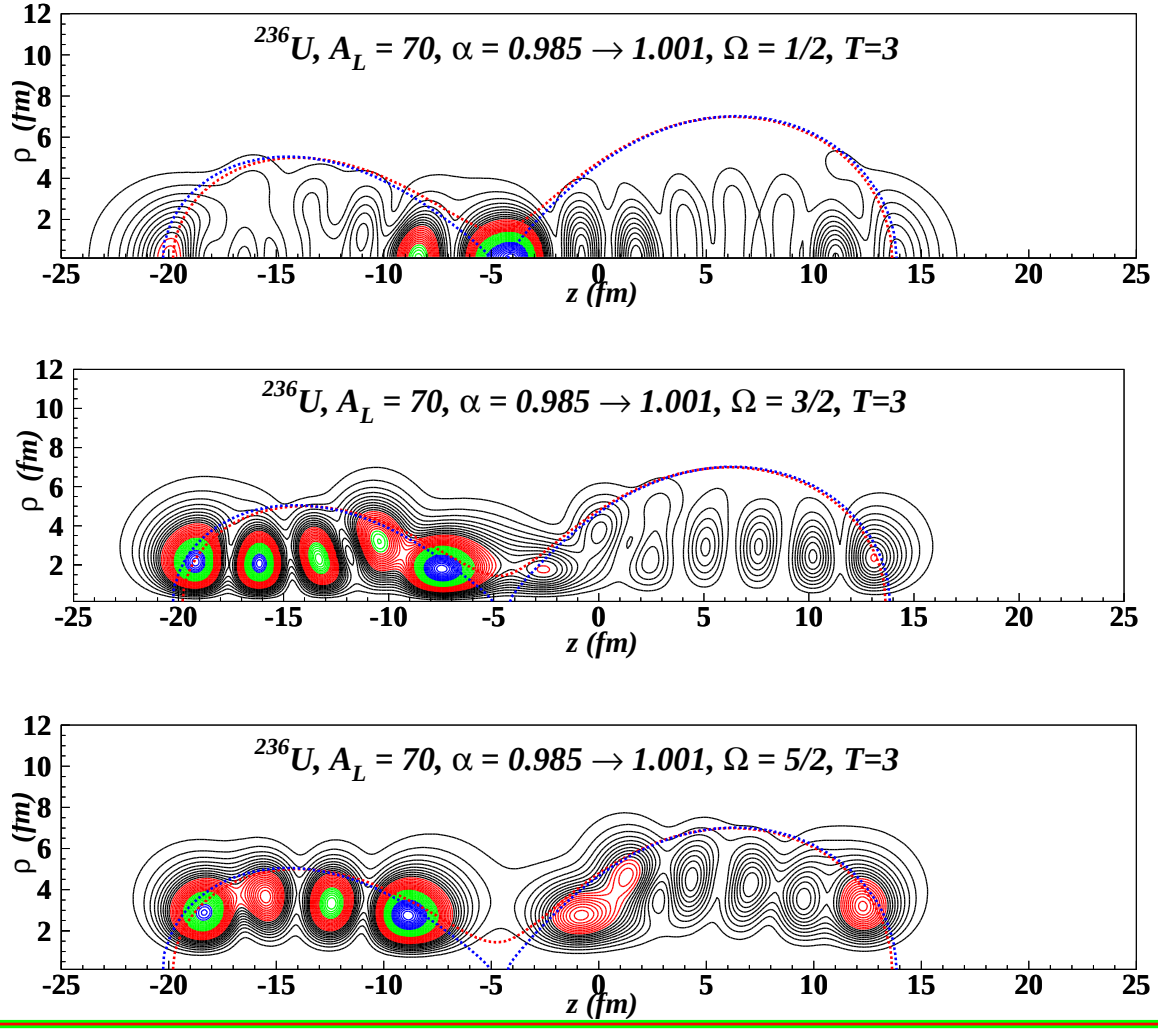

Emission points (A_L=70; T=3; Ω=7/2,9/2,11/2)

For T=3, the distribution of high Ω states is the same as for T=0.

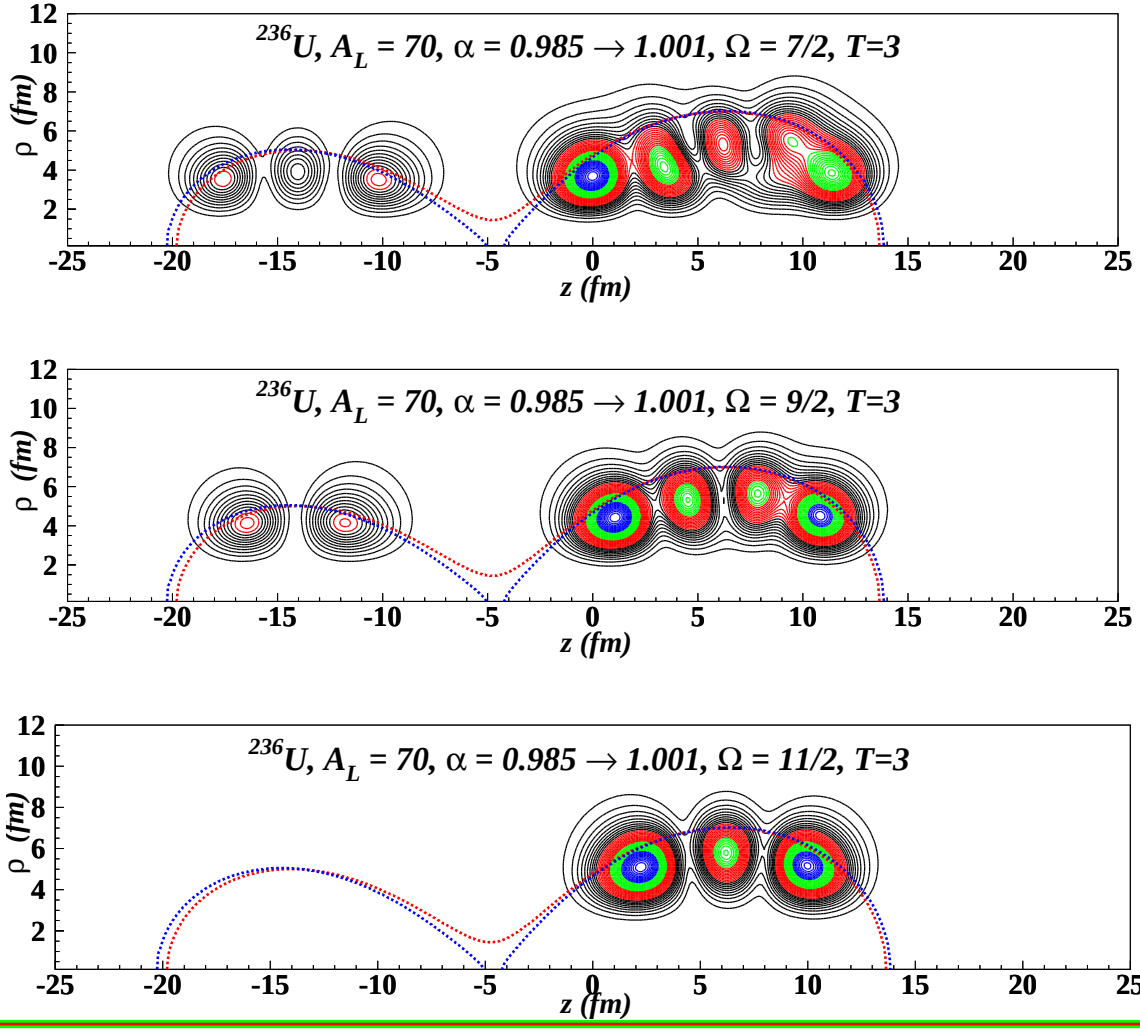

Emission points (A_L=70,86,90,96,118; Ω=3/2; T=0)

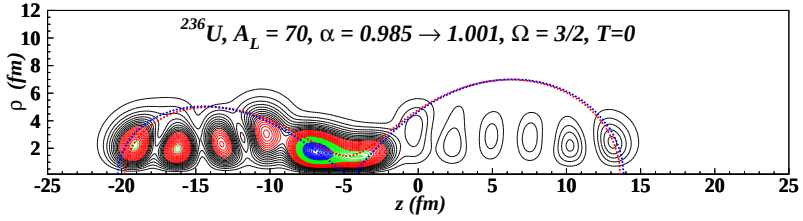

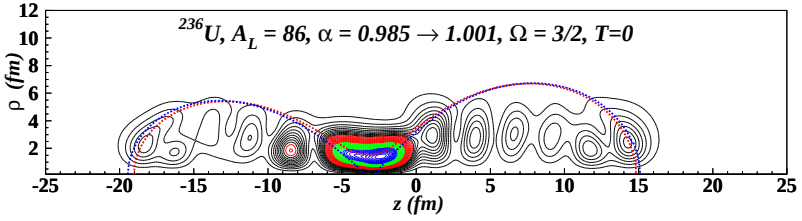

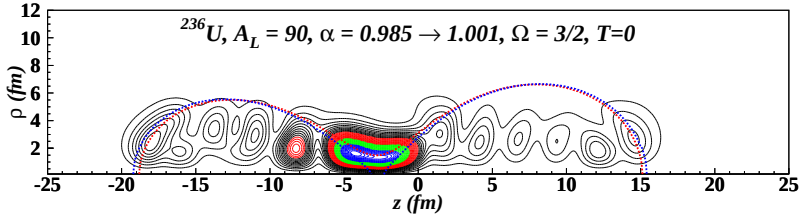

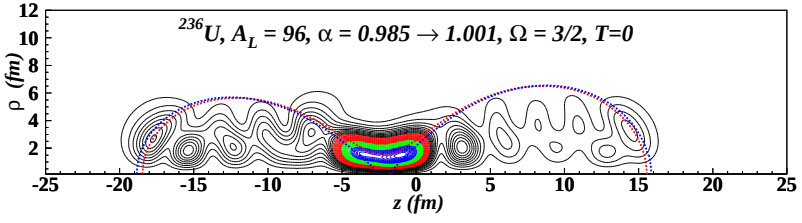

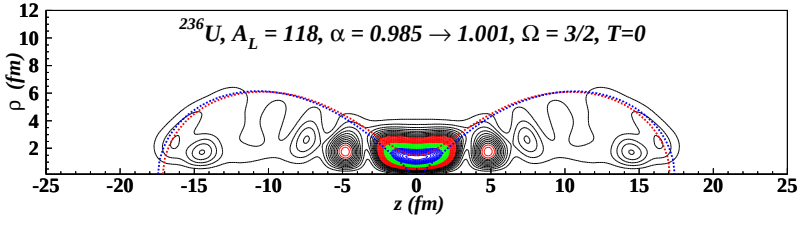

increasing mass asymmetry: monotonous shift towards the L fragment

Emission points (A_L=70,86,90,96,118; Ω=7/2; T=0)

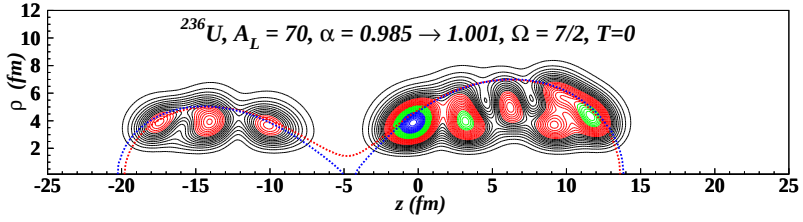

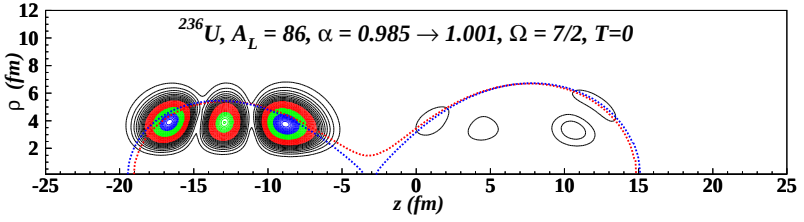

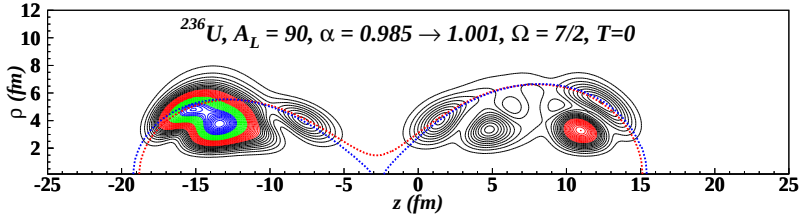

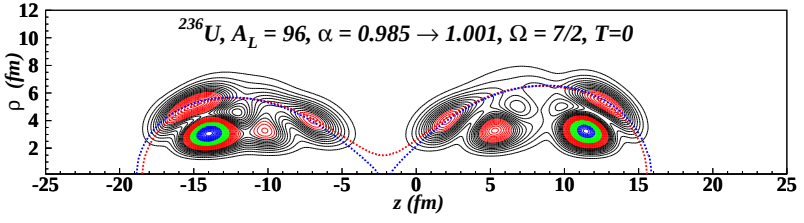

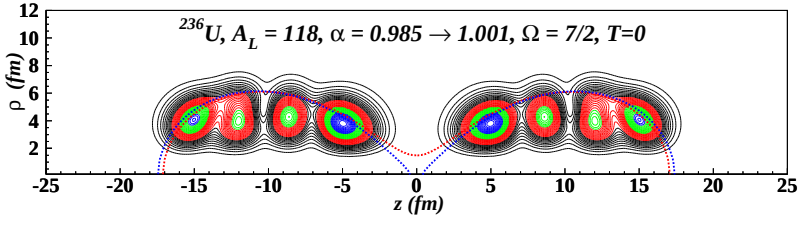

oscillation between L and H fragments

Emission points (A_L=70,86,90,96,118; Ω=9/2; T=0)

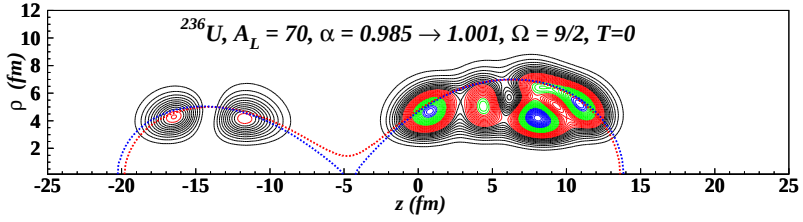

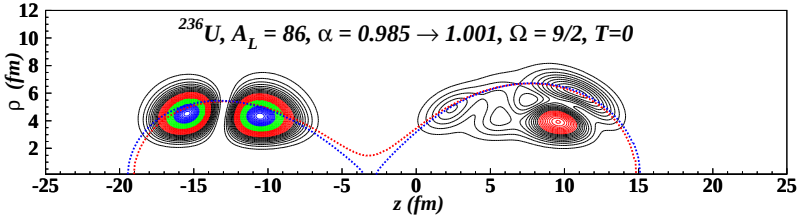

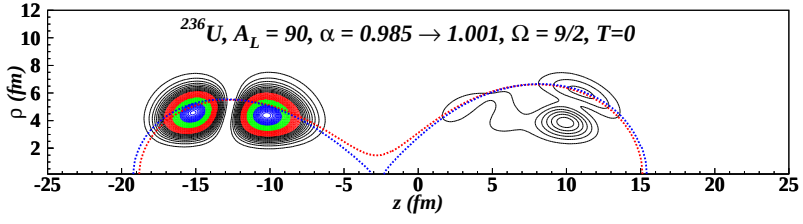

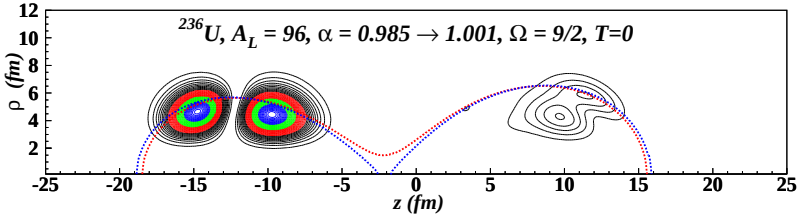

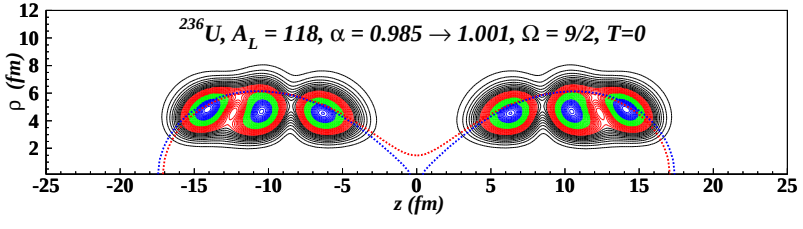

$\nu_{sc}, A_L = 70, A_L/A_H = 0.422, IP(0.985 \rightarrow 1.001)$

T	ν_{sc}	ν_L	ν_H	ν_L/ν_H
0	0.7917	0.3379	0.4538	0.7447
1/2	0.7512	0.3204	0.4308	0.7438
1	0.6682	0.2850	0.3832	0.7439
3	0.2898	0.1222	0.1676	0.7292
5	0.0568	0.0230	0.0338	0.6802
6	0.0184	0.0077	0.0107	0.7104

$\nu_L/\nu_H > A_L/A_H$ *hence the L fragment is more productive*

$\nu_{sc}, A_L = 70, A_L/A_H = 0.422, PC(0.985 \to 1.001)$

T	ν_{sc}	ν_L	ν_H	ν_L/ν_H
0	0.7912	0.3694	0.4218	0.8759
1/2	0.7514	0.3514	0.4000	0.8785
1	0.6701	0.3147	0.3554	0.8854
3	0.3030	0.1426	0.1604	0.8893
5	0.0798	0.0371	0.0427	0.8696
6	0.0434	0.0211	0.0223	0.9468

$\nu_{sc}, A_L = 86, A_L/A_H = 0.573, IP(0.985 \to 1.001)$

T	ν_{sc}	ν_L	ν_H	ν_L/ν_H
0	0.7147	0.3169	0.3978	0.7966
1/2	0.6736	0.2986	0.3750	0.7962
1	0.5928	0.2633	0.3295	0.7990
3	0.2523	0.1144	0.1379	0.8299
5	0.0493	0.0230	0.0263	0.8750
6	0.0155	0.0075	0.0081	0.9271

ν_L/ν_H *increases slightly with T*

$\nu_{sc}, A_L = 86, A_L/A_H = 0.573, PC(0.985 \to 1.001)$

T	ν_{sc}	ν_L	ν_H	ν_L/ν_H
0	0.7088	0.3248	0.3840	0.8459
1/2	0.6683	0.3065	0.3618	0.8472
1	0.5885	0.2710	0.3175	0.8536
3	0.2540	0.1203	0.1337	0.8991
5	0.0541	0.0264	0.0277	0.9555
6	0.0198	0.0099	0.0099	0.9988

$E^*_{sc}, A_L = 86, A_L/A_H = 0.573, IP(0.985 \to 1.001)$

T	E^*_{sc}	E^*_L	E^*_H	E^*_L/E^*_H
0	12.11	6.444	5.670	1.137
1/2	11.60	6.154	5.444	1.130
1	10.52	5.545	4.978	1.114
3	5.300	2.476	2.824	0.8766
5	1.557	0.296	1.261	0.2348
6	0.845	-0.073	0.919	

E^*_L/E^*_H decreases with T: it starts > 1 and ends < 1

$\nu_{sc}, A_L = 90, A_L/A_H = 0.616, IP(0.985 \to 1.001)$

T	ν_{sc}	ν_L	ν_H	ν_L/ν_H
0	0.8333	0.4264	0.4070	1.048
1/2	0.7899	0.4051	0.3848	1.053
1	0.7039	0.3632	0.3406	1.066
3	0.3213	0.1734	0.1479	1.172
5	0.0721	0.0423	0.0298	1.419
6	0.0248	0.0149	0.0099	1.513

ν_L/ν_H *increases with T*

$\nu_{sc}, A_L = 90, A_L/A_H = 0.616, PC(0.985 \rightarrow 1.001)$

T	ν_{sc}	ν_L	ν_H	ν_L/ν_H
0	0.7807	0.3658	0.4149	0.8815
1/2	0.7386	0.3459	0.3927	0.8808
1	0.6557	0.3073	0.3485	0.8819
3	0.2981	0.1427	0.1555	0.9180
5	0.0750	0.0368	0.0382	0.9653
6	0.0348	0.0161	0.0187	0.8574

the initial occupation probabilities influences both the absolute value of ν_L/ν_H *and the magnitude of its increase*

$E^*_{sc}, A_L = 90, A_L/A_H = 0.616, PC(0.985 \rightarrow 1.001)$

T	E^*_{sc}	E^*_L	E^*_H	E^*_L/E^*_H
0	12.20	7.449	4.756	1.566
1/2	11.68	7.162	4.521	1.584
1	10.60	6.569	4.033	1.629
3	5.360	3.648	1.711	2.132
5	1.557	1.584	-0.0262	
6	0.819	1.212	-0.392	

$E^*_L/E^*_H > 1$ *and increases with T; hence L fragment is always more excited*

$\nu_{sc}, A_L = 96, A_L/A_H = 0.686, IP(0.985 \to 1.001)$

T	ν_{sc}	ν_L	ν_H	ν_L/ν_H
0	0.7269	0.3735	0.3534	1.057
1/2	0.6846	0.3525	0.3322	1.061
1	0.6012	0.3109	0.2902	1.071
3	0.2545	0.1328	0.1217	1.091
5	0.0500	0.0249	0.0251	0.990
6	0.0164	0.0079	0.0085	0.936

again $\nu_L/\nu_H > A_L/A_H$ *and slightly increases with T*

$\nu_{sc}, A_L = 96, A_L/A_H = 0.686, PC(0.985 \to 1.001)$

T	ν_{sc}	ν_L	ν_H	ν_L/ν_H
0	0.7077	0.3691	0.3386	1.090
1/2	0.6660	0.3482	0.3178	1.096
1	0.5843	0.3072	0.2771	1.109
3	0.2473	0.1317	0.1156	1.139
5	0.0510	0.0259	0.0250	1.037
6	0.0189	0.0093	0.0096	0.972

$E^*_{sc}, A_L = 96, A_L/A_H = 0.686, IP(0.985 \rightarrow 1.001)$

T	E^*_{sc}	E^*_L	E^*_H	E^*_L/E^*_H
0	13.46	6.276	7.182	0.8738
1/2	12.92	5.996	6.926	0.8658
1	11.80	5.415	6.389	0.8477
3	6.356	2.531	3.825	0.6618
5	2.329	0.4094	1.920	0.2133
6	1.525	0.0079	1.517	0.0052

E^*_L/E^*_H *decreases with T and is always* < 1 *hence H fragment is always more excited*

$E^*_{sc}, A_L = 96, A_L/A_H = 0.686, PC(0.985 \to 1.001)$

T	E^*_{sc}	E^*_L	E^*_H	E^*_L/E^*_H
0	13.16	6.718	6.441	1.043
1/2	12.63	6.439	6.186	1.041
1	11.52	5.862	5.654	1.037
3	6.125	3.006	3.119	0.9637
5	2.165	0.921	1.244	0.7403
6	1.379	0.528	0.851	0.6209

Ratio $\nu_{sc}^{L}/\nu_{sc}^{H}$